Biological Sciences Scholarship   Biological Sciences

5-15-2019

From Spinning Silk to Spreading Saliva: Mouthpart Remodeling in Manduca sexta (Lepidoptera: Sphingidae)

Istvan Miko
University of New Hampshire - Main Campus, istvan.miko@unh.edu

Sarthok Rasique Rahman
Pennsylvania State University

Anne C. Jones
Pennsylvania State University

Mark A. Townley
University of New Hampshire, mark.townley@unh.edu

Brandon Gominho
Pennsylvania State University

See next page for additional authors

Follow this and additional works at: https://scholars.unh.edu/biosci_facpub

Part of the Developmental Biology Commons, and the Entomology Commons

Recommended Citation

Authors

Istvan Miko, Sarthok Rasique Rahman, Anne C. Jones, Mark A. Townley, Brandon Gominho, Sulav Paudel, S David Stupski, Heather M. Hines, and Rudolf J. Schilder

OXFORD

Morphology and Ontology

From Spinning Silk to Spreading Saliva: Mouthpart Remodeling in *Manduca sexta* (Lepidoptera: Sphingidae)

István Mikó,[1,5,] **Sarthok Rasique Rahman,**[2] **Anne C. Jones,**[3] **Mark A. Townley,**[4] **Brandon Gominho,**[3] **Sulav Paudel,**[3] **S. David Stupski,**[2] **Heather M. Hines,**[2,3] **and Rudolf J. Schilder**[2,3]

[1]Department of Biological Sciences, University of New Hampshire, Durham, NH, [2]Department of Biology, Pennsylvania State University, University Park, PA, [3]Department of Entomology, Pennsylvania State University, University Park, PA, [4]University Instrumentation Center, University of New Hampshire, Durham, NH, and [5]Corresponding author, e-mail: istvan.miko@gmail.com

Abstract

As a model organism, the tobacco hornworm *Manduca sexta* (Linnaeus 1763) has contributed much to our knowledge of developmental processes in insects, and major developmental changes between different larval instars are generally well understood. Second and later instars of *M. sexta* do not produce silk, and their spinneret and accessory labial glands (=Lyonet's glands), structures thought to be key players in silk production in other lepidopterans, are highly reduced. To our knowledge, mouthparts and labial gland morphology of the silk-producing first instar have never been described. In this study, we compared the mouthpart morphology and transcriptome profile of first and later instars of *M. sexta* to determine whether the loss of silk production correlates with changes in the structure of the spinneret and the labial glands, and with changes in expression of silk-related genes. We found that the first instar, unlike later instars, has a typical, silk-producing spinneret with a tube-like spigot and well developed Lyonet's glands. Moreover, three known silk protein genes are highly expressed in the first instar but exhibit little to no expression in the embryo or later instars. Thus, the changes in morphology and gene expression presented here, coinciding with changes in larval behavior from silk production to saliva spreading, further our understanding of the developmental processes underlying this transition in this model organism.

Key words: transcriptomics, labial gland, Lyonet's gland, Filippi's gland, spinneret

Manduca sexta (Linnaeus 1763), the tobacco hornworm, is an important pest, and model organism and was the sixth most studied insect species between 1970 and 2016 (Cao and Jiang 2017). The large and relatively easy-to-handle caterpillars of *M. sexta* have been the subject of numerous classic entomological studies related to insect hormones (Rountree and Bollenbacher 1986), cuticle formation (Rebers and Riddiford 1988), immune reaction (Kanost et al. 2016), and nervous system development (Tolbert et al. 1983). Presently, a rich pool of genomic and transcriptomic information is available for *M. sexta* (Cao and Jiang 2015, 2017; Kanost et al. 2016), allowing researchers to reveal relationships between form and function.

Lepidopteran larval labial glands (=salivary glands, silk glands) have been the focus of genomic studies recently as these structures are involved in a wide variety of functions including digestion, detoxification, immunity, herbivore offense (Rivera-Vega et al. 2017a, b), and silk production (Fang et al. 2015). The paired and elongate labial glands of larval insects open into a common duct between the labium (median appendage of the head, ventral to the oral foramen)

and the hypopharynx (anteriormost portion of the alimentary canal that is continuous with the pharynx). In Amphiesmenoptera (Trichoptera+Lepidoptera), the labium and the hypopharynx cannot be differentiated, together forming the labio-hypopharyngeal lobe, and the common duct of the labial glands opens at the tip of the lobe (lb: Fig. 1). In most silk-producing Lepidoptera species (most 'Neolepidoptera', Kristensen 1999, Fedič et al. 2002), a pair of smaller accessory glands, the Lyon(n)et's (or F(Ph)ilippi's) glands, branch from the main gland lumen (Fig. 2D, Helm 1876, Paudel et al. 2018). Although the labial glands are considered the main source of silk proteins, the small Lyonet's glands are also thought to function in silk production given their transcriptomic and secretomic profiles (Wang et al. 2016, 2019).

The area between the highly reduced labial palps on the distal margin of the labio-hypopharyngeal lobe is commonly called the spinneret in Lepidoptera (spin: Fig. 1, Ripley 1924). The labial glands open on a tubular, well-sclerotized structure, the spigot (sp: Fig. 1), that is located medially on the spinneret. The spigot plays a crucial role in
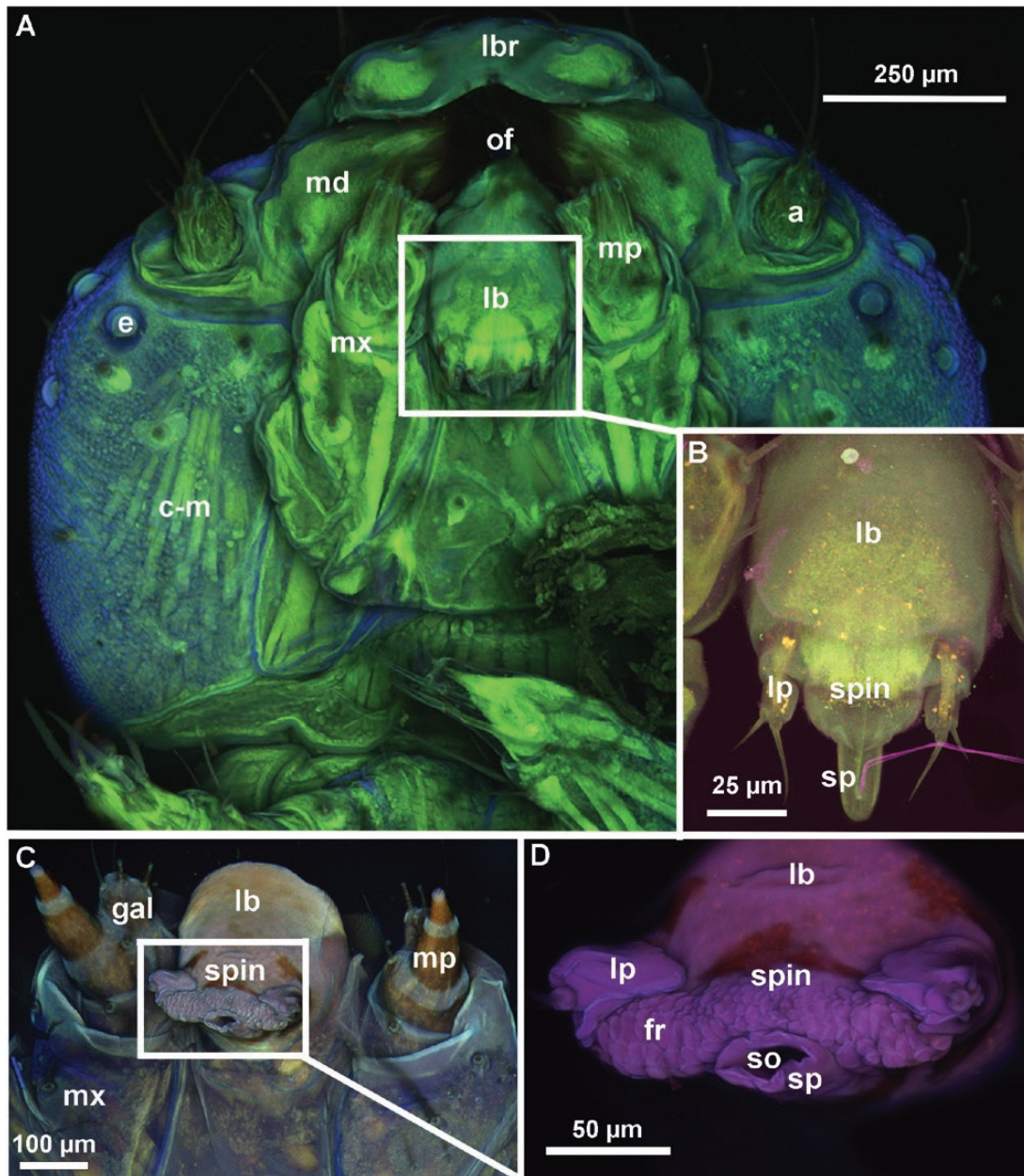
Fig. 1. Labio-hypopharyngeal lobe of first (A, B) and third (C, D) instar larvae of *Manduca sexta*. The labio-hypopharyngeal lobe (lb) forms the ventral wall of the oral foramen (of) and is adjacent to the maxillae (mx) laterally. The spinneret (spin) is the apicomedian portion of the lobe medial to labial palpi (lp) and the sclerotized spigot (sp) is the distalmost part of the common duct of the labial glands bearing the salivary orifice (so). The spinneret is smooth and the spigot protrudes from the apicomedian margin of the spinneret in the first instar (A, B) while the spinneret is equipped with a fringe of hollow, spinelike evaginations (fr) and the spigot does not protrude from the spinneret in later (C, D) instars (a = antenna, cm = mandibular adductor muscle, e = eye, gal = galea, lbr = labrum, lp = labial palp, md = mandible, mp = maxillary palp).

the self-organization of the silk fiber (Ripley 1924, Wang et al. 2016), exhibiting a morphology highly specialized for this function. The spinneret represents perhaps the most anatomically diverse system in lepidopteran larvae on the intra- and interspecific levels and serves as a simple and important model for understanding relationships between form and function (Ripley 1924, MacKay 1964). For instance, the spigot is elongate in silk-producing instars and short in instars that do not produce silk (Ripley 1924, Sorensen et al. 2006) while the spinneret bears a brush-like apical fringe in non-silk-producing instars and is smooth in silk-producing larvae (Ripley 1924).

Most studies of saliva- and silk-producing structures in Lepidoptera have focused on the main tract of the labial gland (Vegliante and Hasenfuss 2012) while information on the Lyonet's

gland and the spinneret is restricted to only a handful of studies (Heinrich 1916, Ripley 1924, Sorensen et al. 2006).

Previous studies have suggested that both the spigot and the Lyonet's gland are absent from *M. sexta* (Leslie and Robertson 1973, Kent et al. 1987, Felton et al. 2014). This finding is not surprising as it is well known that later instars of *M. sexta* do not produce silk. The first instar, however, has been reported to be capable of silk production (Reinecke et al. 1980; Goodman et al. 1985, 2001) and thus could potentially harbor the silk-producing structures. To our knowledge, the labial gland and labio-hypopharyngeal lobe of the first instar larva have never been described.

The aim of the present study is to explore the anatomy of the spinneret and labial glands in different *M. sexta* instars and reveal any
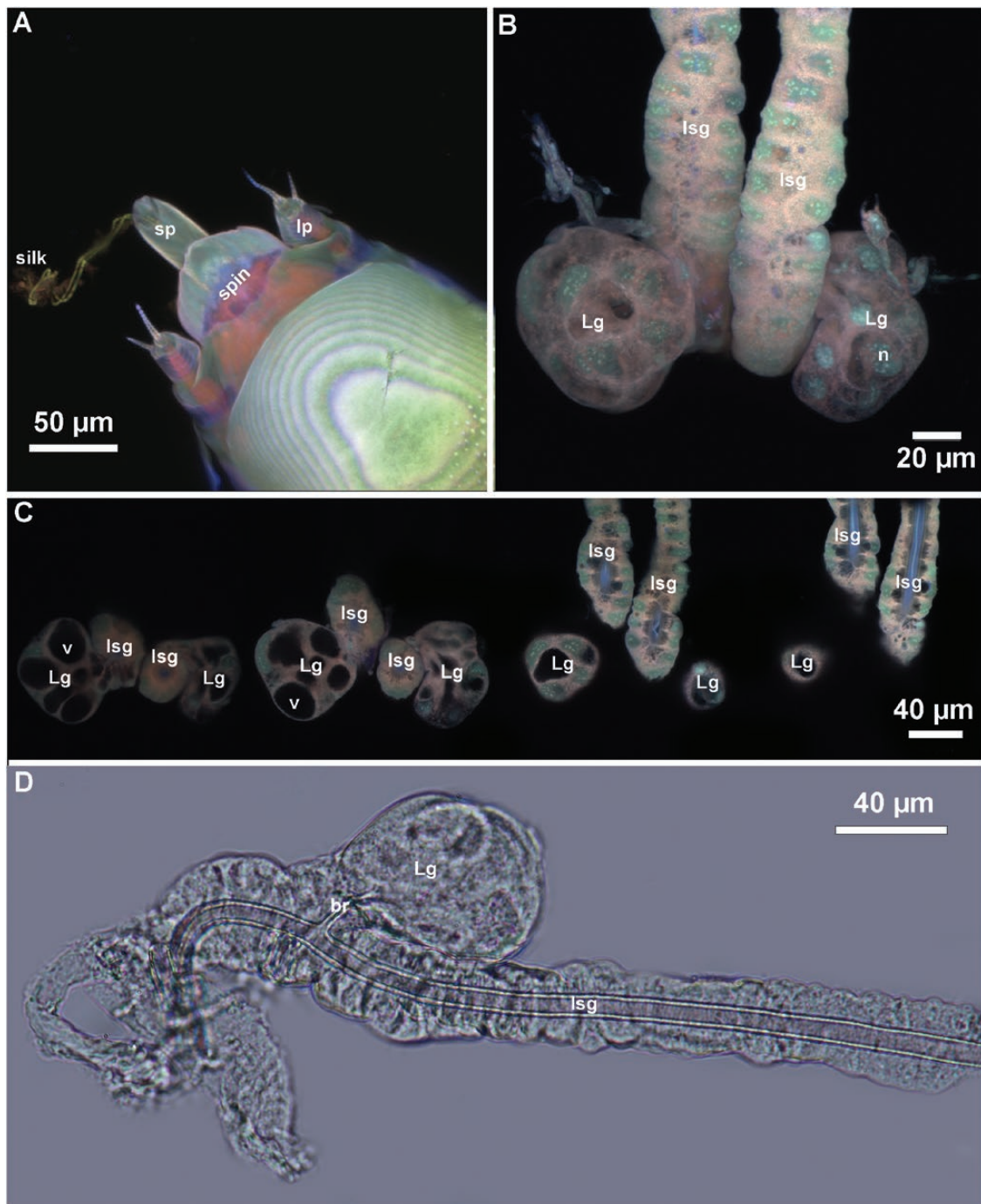
Fig. 2. The labio-hypopharyngeal lobe (A, dorsal view) and the labial gland (B–D) in the first instar larva of *Manduca sexta.* The Lyonet's gland (Lg), is composed of 10–12 epithelial cells surrounding the proximal branch (br) off the main lumen of the labial gland (lsg). The cells of the Lyonet's gland possess enlarged nuclei (n) and are filled with secretory vesicles (v). A, B volume-rendered CLSM micrographs, C CLSM micrographs, D brightfield micrograph (lp = labial palp, sp = spigot, spin = spinneret).

morphological changes between silk-producing and non-silk-producing instars. We also compare available transcriptomes to determine how silk gene expression shifts with changing morphologies in this species.

Materials and Methods

Specimens

First, second, third, fourth, and fifth instars of *M. sexta* were provided by the Andrew Stephenson lab and the Schilder lab at Pennsylvania State University. Larvae were fed on *Nicotiana benthamiana* and an artificial diet for 24 h prior to dissection.

Terminology

Morphological terminology follows Hasenfuss and Kristensen (2003), Ripley (1924), and Godfrey (1972). A list of anatomical terms with their abbreviations used on figures, and synonym terms applied in earlier works, are given in Supp Table 1 (online only). Anatomical terms used in the descriptions are linked to concepts

in the Hymenoptera Anatomy Ontology (HAO; Hymenoptera Anatomy Portal; http://portal.hymao.org).

Microscopy

Specimens were dissected in 0.1 M dibasic phosphate buffer, pH 7.4, using an Olympus SZX 16 stereomicroscope. Labial glands and the labio-hypopharyngeal lobe were fixed in 2.5% glutaraldehyde in 0.1 M dibasic phosphate buffer, pH 7.4, for 24 h at 4°C. Specimens were washed in 0.1 M phosphate buffer (3× 15 min), transferred into anhydrous glycerol, and kept on

concavity slides for further examination. Specimens were imaged between two #1.5 coverslips with an Olympus FV10i confocal laser-scanning microscope (CLSM) at the Microscopy and Cytometry Facility at the Huck Institute of Life Sciences, Pennsylvania State University and with a Nikon A1R-HD CLSM at the University of New Hampshire Instrumentation Center. With the Olympus FV10i we used three excitation wavelengths, 405 nm, 473 nm, and 559 nm, and detected the autofluorescence using two channels with emission ranges of 490–590 nm and 570–670 nm (Fig. 2A–C). On the Nikon A1R-HD, we either used three excitation wavelengths, 409, 487, and 560 nm, and three
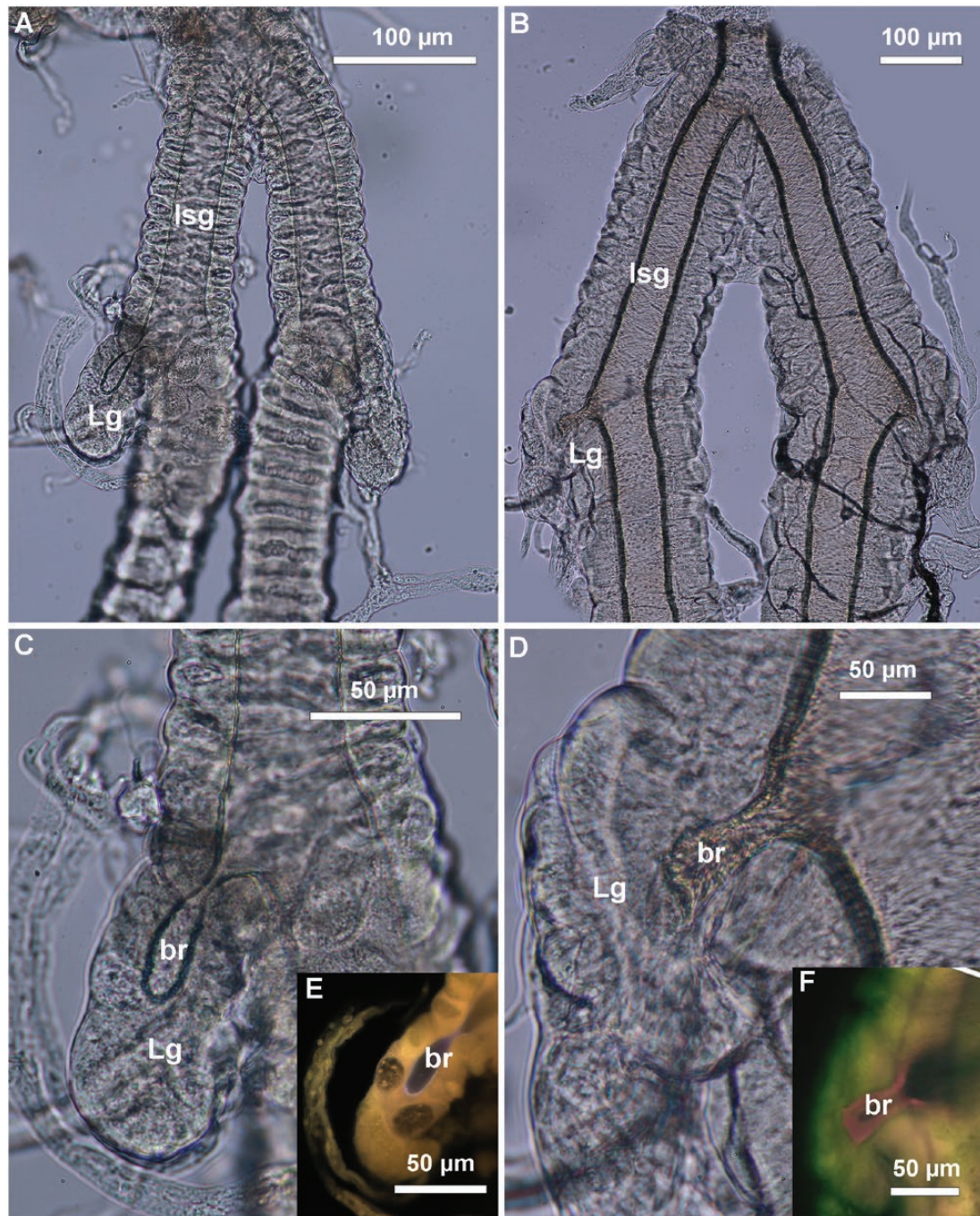

Fig. 3. The Lyonet's and labial glands in second (A, C, E) and third (B, D, F) instar larvae of *Manduca sexta*. The Lyonet's gland (Lg) is larger in the second instar than in the third instar. The chitinized branch (br) of the labial gland (lsg) is apparently closed. The diameter of the epithelial cell cluster composing the Lyonet's gland is less than half the size of the main branch of the labial gland.

emission ranges of 435–470, 500–540, and 570–645 nm (Fig. 1) or used one excitation wavelength, 487 nm, with emission ranges defined using the A1-DUS spectral detector, 500–560 nm and 570–630 nm (Figs. 3E and F and 4–6). The resulting image sets were assigned pseudo-colors that reflected the fluorescence spectra. Volume-rendered micrographs and media files were created using FIJI (Schindelin et al. 2012) and Nikon NIS-Elements AR v. 5.02.01.
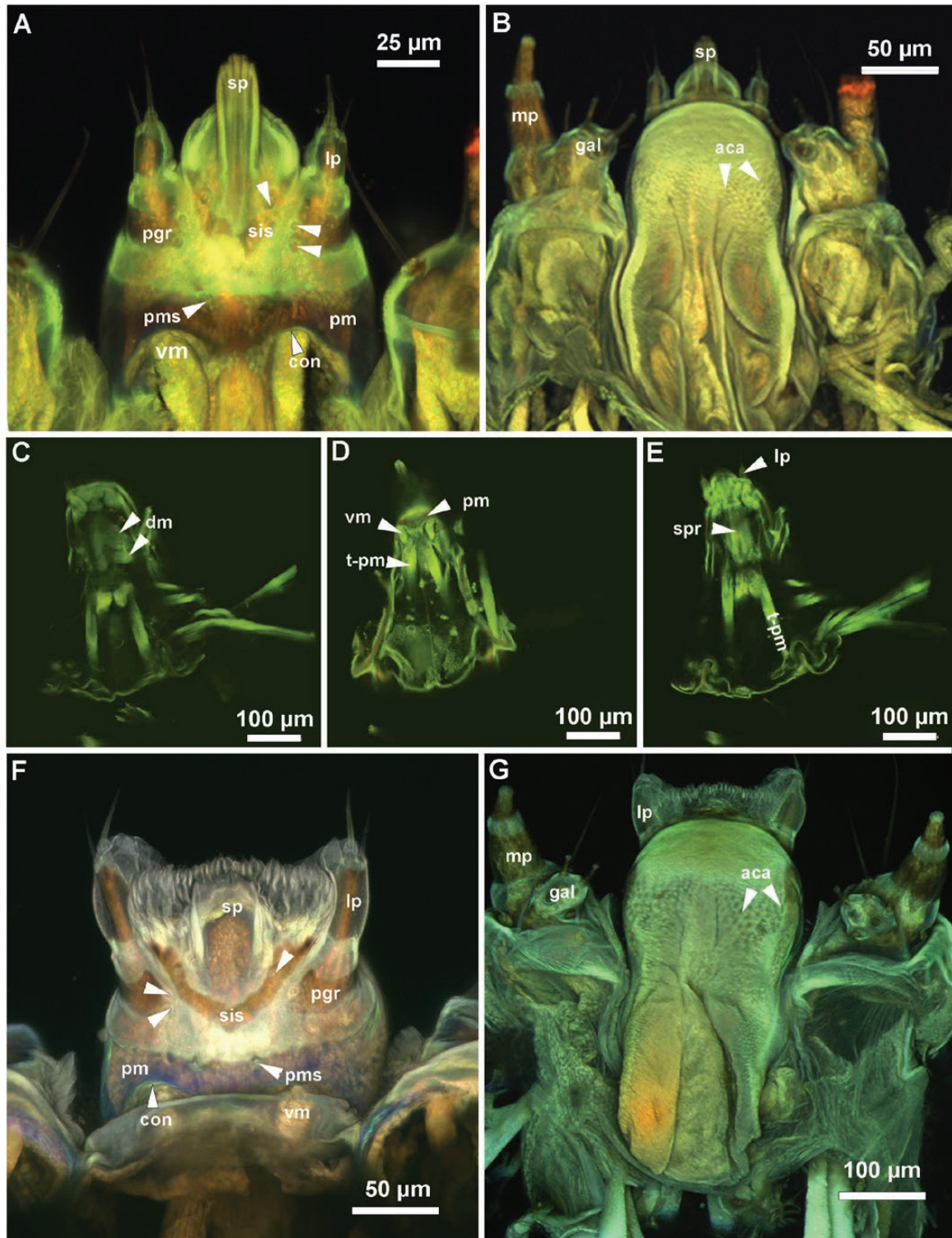

Fig. 4. Labio-hypopharyngeal lobe of first (A–E) and second (F, G) instars of *Manduca sexta*. The spigot (sp) is more than four times as long as wide and clearly protrudes from the convex, sculptureless distal margin of the spinneret in the first instar (A, B) whereas it is almost as wide as long and obscured by the fringed distal margin of the spinneret in later instars (F, G). Two intrinsic (dm, vm) and one extrinsic (t-pm) muscles of the labio-hypopharyngeal lobe have been observed in all instars with similar configuration and relative size. (A) First instar, ventral view. (B) First instar, dorsal view. (C–E) first instar, ventral view. (F) Second instar, ventral view. (G) Second instar, dorsal view (Unlabeled arrowheads in A, F point to campaniform sensilla; arrowheads in C point to the two bands composing dm) (aca = acanthae, con = concavities on posterior premental margin, dm = dorsal premento-salivarial muscle, gal = galea, lp = labial palp, mp = maxillary palp, pgr = palpiger, pm = prementum, pms = premental stipular setae, sis = proximal sclerite of the spinneret, sp = spigot, t-pm = tentorio-premental muscle, vm = ventral premento-salivarial muscle).
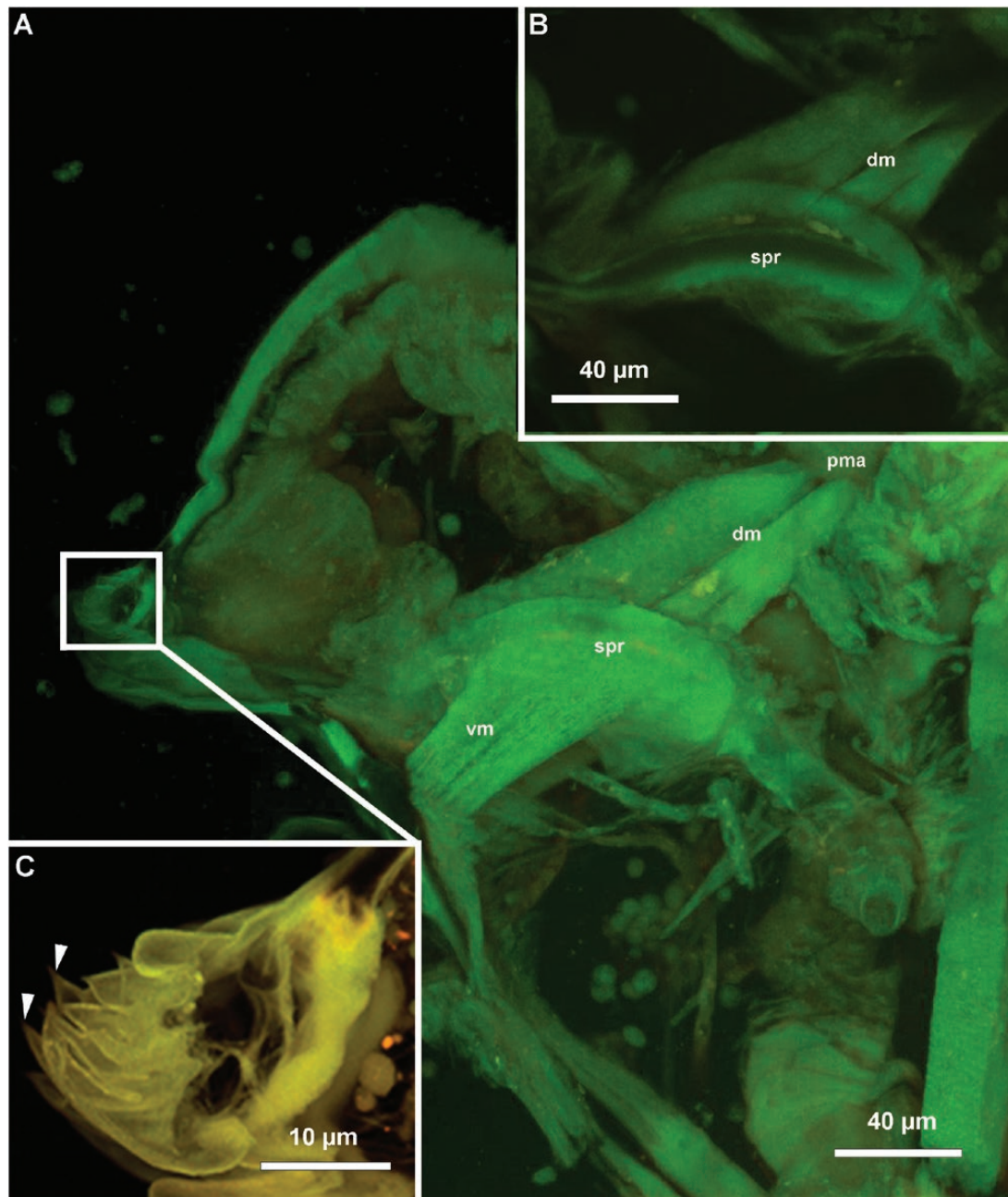
Fig. 5. Labio-hypopharyngeal lobe of the third instar of *Manduca sexta*. The salivarium (=silk press, spr) and its muscles (vm, dm) of second and later instars are similar to those of the first instar, indicating that the structure plays a similar role (closing and opening of the salivary orifice) in the saliva-producing instars and the silk-producing first instar. Starting with the second instar, the distal margin of the spinneret is equipped with hollow cuticular evaginations (arrowheads in C) that form a fringe. This brush-like structure might be involved in saliva spreading (dm = dorsal premento-salivarial muscle, pma = premental arm, spr = salivarium (=silk press), vm = ventral premento-salivarial muscle).

Transcriptomics

To obtain transcriptome profiles of first instar and other developmental stages of *M. sexta*, raw sequencing reads were obtained from published transcriptomics datasets (Cao and Jiang 2017) in the NCBI Sequence Read Archive (SRA) for egg/embryo (SRR2659994) and for first instar (SRR2660019), second instar (SRR2660035), and third instar (SRR2660033) larvae, while sequencing reads for fourth instar larvae were obtained from the authors of a published study (Koenig et al. 2015). The egg/embryo and first through third instar transcriptomes were obtained using whole body extractions (Cao and Jiang 2015), while the fourth instar transcriptome was obtained from the salivary gland only (Koenig et al. 2015). Initial quality assessment of reads was conducted

in FastQC v. 0.11.7 (Andrews 2010) followed by appropriate adaptor trimming and low-quality base trimming in Trimmomatic v. 0.38 (Bolger et al. 2014) using the following parameters: SLIDINGWINDOW:3:30 ILLUMINACLIP:TruSeq3-SE.fa:2:30:10 MINLEN:10. These trimmed reads were used to estimate isoform-level transcript abundance utilizing the Kallisto v. 0.45.0 RNA-seq quantification tool (Bray et al. 2016), with publicly available *M. sexta* assembled transcripts used as the reference (Kanost et al. 2016). TPM-normalized counts obtained from the Kallisto tool (Bray et al. 2016) were merged to produce a gene-level abundance count table (Supp File 1 [online only]).

To identify the silk-producing genes in *M. sexta*, we took a candidate gene approach. We curated a list of silk-producing candidate
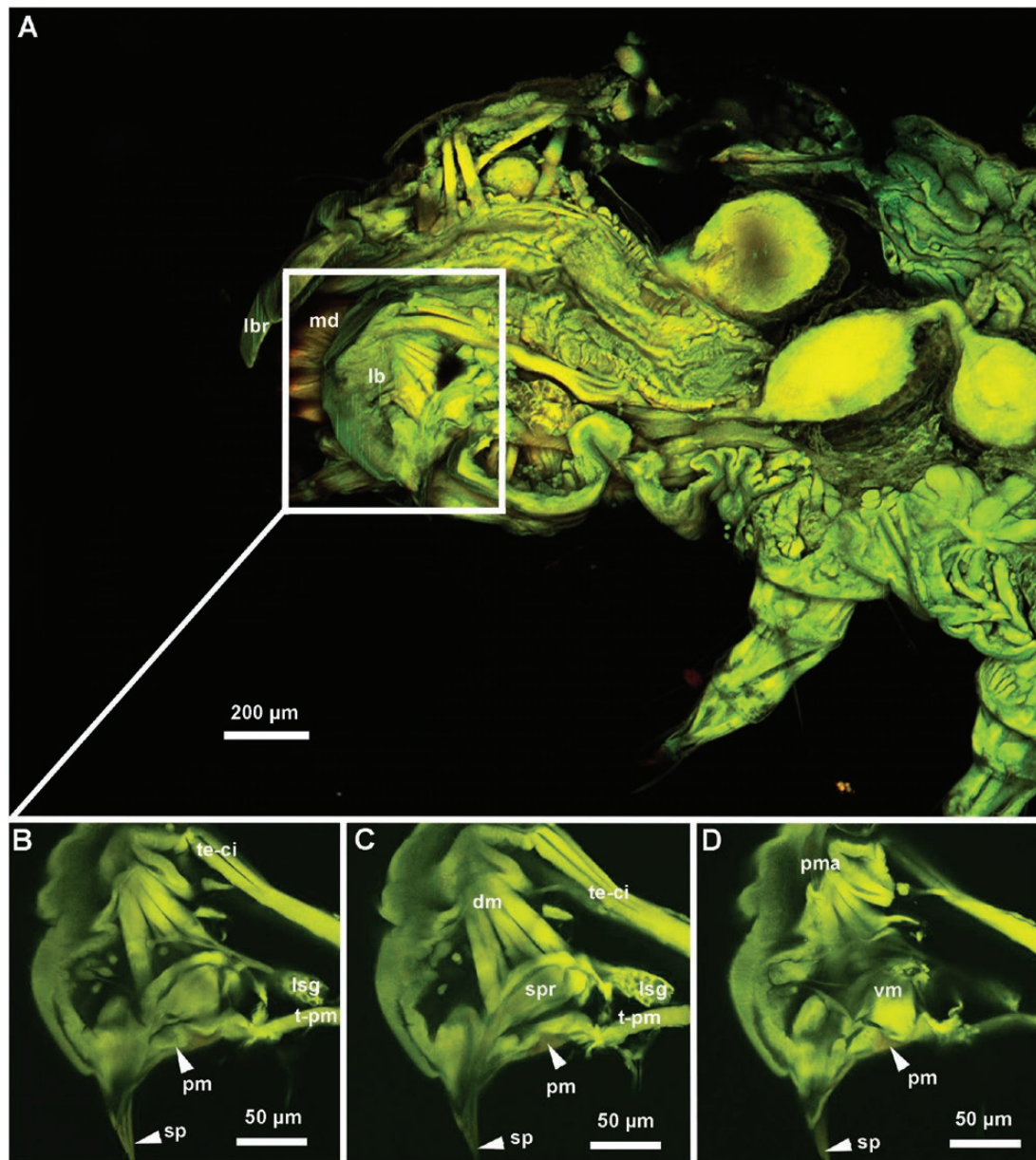
Fig. 6. Labio-hypopharyngeal lobe (lb) of the first instar of *Manduca sexta* (medial views of longitudinal cross sections). The spigot (sp) of the first instar is elongate and cone shaped and is connected to the salivarium (spr) via arthrodial membrane (dm = dorsal premento-salivarial muscle, lb = labio-hypopharyngeal lobe, lbr = labrum, lsg = labial gland, md = mandible, pm = prementum, pma = premental arm, spr = salivarium (=silk press), t-pm = tentorio-premental muscle, te-ci = tentorio-cibarial muscle, vm = ventral premento-salivarial muscle).

genes from the literature (Yamaguchi et al. 1989; Žurovec et al. 1995; Tanaka and Mizuno 2001; Žurovec and Sehnal 2002; Fedič et al. 2003; Yonemura et al. 2006, 2009; Yonemura and Sehnal 2006; Collin et al. 2010; Ou et al. 2014; Huang et al. 2016; Zhou et al. 2016). Transcripts of these genes were obtained from NCBI (see Supp File 2 [online only] for accession numbers and FASTA-format sequences) and we used tblastx from BLAST command line tools (Madden 2002) to obtain the best hits in the *M. sexta* assembled transcriptomes, only accepting hits after applying a stringent E-value of <1e-10. We also obtained top hits of these candidate genes in *Bombyx mori* transcripts to better understand their functions (International Silkworm Genome Consortium 2008).

To identify genes which are highly and differentially expressed in first instar larvae compared to other instars and stages, we isolated those genes that had a normalized read count (TPM) value of at least 20 in the first instar and thus were among the more highly expressed genes, and that had at least a threefold higher level of gene expression in the first instar compared to the egg, second instar, and third instar. This generated 298 genes. We then developed a ranking of these genes to identify the most highly and differentially expressed set of genes by summing read count number + rank of fold difference in gene expression of first instar/egg + rank of fold difference of first instar/second instar + rank of fold difference of first instar/third instar, and sorting by those with the highest rank overall. This list (Supp File 1 [online only]) was used to determine whether silk genes were among the genes with especially high and differential expression in the first instar.

Results

Morphology

In the following section we provide a general description of morphological traits of the proximal region of the labial gland and the musculoskeletal system of the labio-hypopharyngeal lobe of *M. sexta* that are shared with all instars. We summarize differences between the first and later instars in Table 1.

The two labial glands merge anteriorly into a common duct before they reach the salivarium (Fig. 3A and B). The cuticular intima of each gland is branched just posterior to this merging point into a cluster of epithelial cells referred to here as the Lyonet's gland (br, Lg: Figs. 2B–D and 3). The common duct of the labial glands is continuous with the salivarium (=silk press), a dilated extension of this duct with partially sclerotized wall (spr: Figs. 4E, 5A and B, and 6C). The salivarium is connected anteriorly to the spigot (sp: Figs. 1B and D, 2A, 4A, B, and F, and 6B–D), the distalmost part of the common duct of the labial glands that is sclerotized and bears the salivary orifice (so: Fig. 1C and D). The spigot opens just ventral to the apical margin of the labio-hypopharyngeal lobe, the spinneret (spin: Figs. 1B–D and 2A). The spinneret is bounded laterally by the two labial palps (lp: Figs. 1B and D, 2A, and 4A, F, and G) and ventromedially by the proximal sclerite of the spinneret (sis: Fig. 4A and F), which is v-shaped and bears two submedial campaniform sensilla (arrows in Fig. 4A and F). The proximal segment of the labial palp is sclerotized, the distal segment is not. The distal segment has two apical setae. The proximal regions of the labial palps are encircled externally by the palpigers (pgr: Fig. 4A and F) which bear two medial campaniform sensilla (arrows in Fig. 4A and F). The proximal sclerite of the spinneret and the palpigers are connected to the distal margin of the prementum (pm: Fig. 4A, D, and F) by flexible arthrodial membrane. This distal margin is straight while the proximal margin of the prementum is medially extended into a projection that separates two submedial concavities on the posterior premental margin (con: Fig. 4A and F). The prementum has one pair of distomedial setae (pms: Fig. 4A and F, stipular setae). Paired premental arms extend dorsolaterally on the labio-hypopharyngeal lobe (pma: Figs. 5A and 6D). We did not observe any further sclerotization on the dorsal wall of the lobe, which is covered with dense acanthae (aca: Fig. 4B and G) proximally and is smooth distally. The ventral premento-salivarial muscles arise from the arthrodial membrane, limited anteriorly by the submedial concavities on the posterior premental margin, and insert on the ventrolateral region of the salivarium (vm: Figs. 4A, D, and F, 5A, and 6A and D). The dorsal premento-salivarial muscles (dm: Figs. 4C, 5A and B, and 6A and C) arise from the premental arms and are divided into an anterior and a posterior band. These bands insert along

the dorsal side of the salivarium. The tentorio-premental muscles (t-pm: Figs. 4D and E and 6A–C) insert medially at the proximal margin of the prementum and the tentorio-cibarial muscles (te-ci: Figs. 6A–C) insert medially on the dorsal region of the labio-hypopharyngeal lobe. We did not observe any premento-labial palp muscles.

Transcriptomics

In our search for known silk genes in the *M. sexta* transcriptome we found five gene hits. Of these five, three genes—the light-chain fibroin, heavy-chain fibroin, and silk protein P25—were highly expressed in the first instar larva while considerably less expressed outside this instar (Table 2). The other two genes were sericins and exhibited low expression (<1 TPM) across all stages/instars. When we sorted all genes to identify those that are most highly expressed in the first instar, and most differentially expressed between first instars and other stages/instars, these three genes ranked among the set of top 20 most highly and differentially expressed genes (Supp File 1 [online only]).

Discussion

Lyonet's Glands and Spigots are Present in *M. sexta* Larvae

Modifications of the Lepidoptera spinneret and Lyonet's gland between silk-producing and non-silk-producing species and/or instars make these structures feasible models to study how form and function change during the course of both development and evolution (Helm 1876, Ripley 1924, MacKay 1964). Yet, our knowledge of these structures in Sphingidae, including *M. sexta*, is surprisingly limited. Leslie and Robertson (1973) described the labial glands of later instars of *M. sexta*, but did not mention the Lyonet's glands, which, though reduced in size, are still present in later instars (Fig. 3). The reduced gland was illustrated in Hakim (1976) and Peterson (1912), but neither author mentioned this structure in their descriptions. The only accurate illustration and description of the reduced Lyonet's gland in later instars of Sphingidae was provided in the 19th century by Helm (1876). However, silk production has never been observed in later instars of any sphingids and we found that established silk genes (two fibroins and silk protein P25) are only expressed in the first instar of *M. sexta*. Thus, the reduced Lyonet's glands of second and later instars are most likely not involved in silk production. Further examination is needed to determine whether they have any new functions in later instars or if they represent vestigial structures.

Table 1. Differences in morphology of first and later instars of *M. sexta*

Morphological trait	First instar	Later instars
Spigot length	Four times as long as wide, protruding beyond distal margin of spinneret, exceeding apical ends of labial palps	1–1.5 times as long as wide, not protruding beyond distal margin of spinneret, not exceeding apical ends of labial palps
Spigot apical margin shape	Conical	Square
Shape of spinneret area between labial palps	Convex	Straight
Hollow apical projections on spinneret composing a brush	Absent	Present (Fig. 5C)
Number of cells forming each Lyonet's gland	Around 10	3–4
Secretory vesicles in cells forming Lyonet's gland	Present	Absent
Diameter of Lyonet's gland vs width of main labial gland duct	2X	0.5X

Table 2. Silk-producing genes in *Manduca sexta* identified by candidate gene approach and their expression level in egg/embryo and in 1st, 2nd, 3rd, and 4th instar larvae (in TPM)

Gene	*M. sexta* ID	Egg/embryo	1st	2nd	3rd	4th
Light-chain fibroin (*Fib-L*)	Msex2.08837	0	272.30	0.54	0	5.47
Heavy-chain fibroin (*Fib-H*)	Msex2.10750	0	57.46	0	0	0
Silk protein P25 (*P25*)	Msex2.05964	0	68.06	0	0	0
Sericin 2 (*Ser2*)	Msex2.06479	0	0.44	0.04	0.10	0.82
Sericin 3 (*Ser3*)	Msex2.11225	0.71	0	0	0	0

According to Forbes (1910) and Ripley (1924), who provided very limited information on the spinneret of later instars in Sphingidae, the spinneret is broad, flat, short, fringed, and basally equipped with three sclerites. The only illustration of the spinneret of *M. sexta* was published by Rivera-Vega et al (2017b). We provide the first detailed description of the musculoskeletal system of the labio-hypopharyngeal lobe for *M. sexta* and show that, although first instar morphology is distinct from that of later instars, this difference is restricted to the external morphology of the spinneret. The first instar spinneret is similar to that of the silk-producing caterpillars as it has an elongate, conical spigot and a sculptureless apical margin. In later instars, although present, the spigot is much shorter and it is obscured by hollow, conical cuticular evaginations that form a brush-like structure.

Remodeling of the Spinneret

The spigot of the first instar extends apically beyond the labial palps and the apical margin of the spinneret is sculptureless, while later instars have a flat spinneret that is equipped with hollow, pointed evaginations that resemble a brush and obscure the short spigot. This type of radical remodeling has not been previously reported in Lepidoptera spinnerets. The size of a spigot is correlated with the amount of silk produced, but it usually changes gradually during the course of development (Ripley 1924, Sorensen et al. 2006). Ripley (1924) recognized four different developmental trajectories in spigot morphology. In the first type, the spigot is longest in the first and last instars and somewhat shorter in intermediate instars. Species belonging to this group produce the most silk during their first and last larval instars. In the second type, the first instar possesses a long spigot that then gradually shortens in successive larval instars, while in the third type, the spigot is short in the first instar and gradually grows and reaches its maximum length in the final instar. In these types, only the instars with the longest spigots produce silk. In the fourth type, the spinneret remains short and none of the instars produce silk. Instead, a fringe develops gradually on the apical margin of the spinneret. Ripley (1924) classified Sphingidae into the fourth type.

The salivarium and its ventral and dorsal premento-salivarial muscles are well developed in all instars. The former structure is often referred to as the 'silk press'. Hinton (1958) demonstrated that silk is not pressed out by this organ, but drawn out by the movements of the head after the silk is fastened on a surface. The silk press and adjacent muscles regulate silk extrusion by closing and opening the lumen of the salivarium and are hypothesized to shear the silk (Sorensen et al. 2006). Shearing might be an important process in generating the optimal mechanical properties of the silk. The relative size of the salivarium and its musculature does not change radically between the first and later instars, indicating that the opening and closing function of the salivarium is still used while the labial glands are exclusively producing saliva.

Possible Silk Functions in *M. sexta*

First instar larvae of *M. sexta* produce two kinds of silk structures: silk strands on which they descend and silk pads on which they fix themselves with their prolegs before they molt (Reinecke et al. 1980; Goodman et al. 1985, 2001). In this study, we observed first instar larvae producing silk pads even on artificial substrates (Supp Fig. 1 [online only]), but we did not observe them creating silk strands and descending using them. The timing of silk pad deposition indicates that the first instar larva needs the pad for proper molting. Descending on silk strands can serve multiple major functions in lepidopterans, such as dispersal (Diss et al. 1996), changing position within the same plant (Torres-Vila et al. 1997), and defensive drop-off (Perović et al. 2008). These behaviors are often observed only in neonate larvae as later instars may be too heavy to use silk strands for these purposes (Hagstrum and Subramanyam 2010).

Silk Production Versus Digestion: Morphology and Transcriptomics

The caterpillar's labial gland secretions are potentially involved in numerous physiological mechanisms such as digestion, detoxification, and suppression of host plant immunity (Rivera-Vega et al. 2017a, b). These secretions are likely deposited on the plant surface before the ingestion of plant material. The tubular spigot shape of silk-producing Lepidoptera larvae is highly specialized for drawing silk (Sorensen et al. 2006, Wang et al. 2016) and likely is not as efficient for distributing saliva. Besides Sphingidae, brush-like spinnerets can be found in some noctuid taxa that pupate in the soil. It has been hypothesized that the labial brush is used to distribute saliva in the soil chamber to stabilize and waterproof its wall (Ripley 1924). Although *M. sexta* pupate in a soil chamber, the fully developed spinneret brush appears already in the second instar larva. Thus, *M. sexta* larvae may be using the brush-type spinneret to distribute saliva on the plant surface, increasing the efficacy of enzymes involved in digestion and detoxification.

Spinneret remodeling in *M. sexta* coincides with a reduction of the Lyonet's glands (cf. Figs. 2 and 3) that reportedly play an important role in silk production (Wang et al. 2016, 2019). The shift in function from silk to saliva production indicated by these morphological changes was supported by stage/instar-specific shifts in gene expression. In our comparison of embryo and larval transcriptomes of *M. sexta*, we found three silk genes (light- and heavy-chain fibroins and silk glycoprotein P25) whose expression is largely confined to the first instar, and found that these were among the top genes with high and differential expression exclusive to this instar. These proteins are the main three components of a silk fiber and are expressed in high amounts during silk production (Inoue et al. 2000). The adhesive sericin that usually coats these fibers is largely absent in the first instar *Manduca* larvae, suggesting it is less important for first instar silk production. Together the orchestrated remodeling of the spinneret and labial glands, and changes in the transcriptome profile, suggest an abrupt change in larval behavior in *M. sexta* from silk production to digestion and detoxification.

Supplementary Data

Supplementary data are available at *Insect Systematics and Diversity* online.

Acknowledgments

References Cited

Andrews, S. 2010. FastQC: a quality control tool for high throughput sequence data. http://www.bioinformatics.babraham.ac.uk/projects/fastqc.

Bolger, A. M., M. Lohse, and B. Usadel. 2014. Trimmomatic: a flexible trimmer for illumina sequence data. Bioinformatics. 30: 2114–2120.

Bray, N. L., H. Pimentel, P. Melsted, and L. Pachter. 2016. Near-optimal probabilistic RNA-seq quantification. Nat. Biotechnol. 34: 525.

Cao, X., and H. Jiang. 2015. Integrated modeling of protein-coding genes in the *Manduca sexta* genome using RNA-Seq data from the biochemical model insect. Insect. Biochem. Mol. Biol. 62: 2–10.

Cao, X., and H. Jiang. 2017. An analysis of 67 RNA-seq datasets from various tissues at different stages of a model insect, *Manduca sexta*. BMC Genomics 18: 796.

Collin, M. A., K. Mita, F. Sehnal, and C. Y. Hayashi. 2010. Molecular evolution of lepidopteran silk proteins: insights from the ghost moth, *Hepialus californicus*. J. Mol. Evol. 70: 519–529.

Diss, A. L., J. G. Kunkel, M. E. Montgomery, and D. E. Leonard. 1996. Effects of maternal nutrition and egg provisioning on parameters of larval hatch, survival and dispersal in the gypsy moth, *Lymantria dispar* L. Oecologia. 106: 470–477.

Fang, S.-M., B.-L. Hu, Q.-Z. Zhou, Q.-Y. Yu, and Z. Zhang. 2015. Comparative analysis of the silk gland transcriptomes between the domestic and wild silkworms. BMC Genomics 16: 60.

Fedič, R., M. Žurovec, and F. Sehnal. 2002. The silk of Lepidoptera. J. Insect Biotechnol. Sericol. 71: 1–15.

Fedič, R., M. Žurovec, and F. Sehnal. 2003. Correlation between fibroin amino acid sequence and physical silk properties. J. Biol. Chem. 278: 35255–35264.

Felton, G. W., S. H. Chung, M. G. E. Hernandez, J. Louis, M. Peiffer, and D. Tian. 2014. Herbivore oral secretions are the first line of protection against plant-induced defences. Annual Plant Reviews. 47: 37–76.

Forbes, W. T. M. 1910. A structural study of some caterpillars. Ann. Entomol. Soc. Am. 3: 94–132.

Godfrey, G. L. 1972. A review and reclassification of larvae of the subfamily Hadeninae (Lepidoptera, Noctuidae) of America north of Mexico. Technical Bulletin. US Department of Agriculture. 1450: 1–265.

Goodman, W. G., R. O. Carlson, and K. L. Nelson. 1985. Analysis of larval and pupal development in the tobacco hornworm (Lepidoptera: Sphingidae), *Manduca sexta*. Ann. Entomol. Soc. Am. 78: 70–80.

Goodman, W. G., R. Jeanne, and P. Sutherland. 2001. Teaching about behavior with the tobacco hornworm. The American Biology Teacher. 63: 258–261.

Hagstrum, D. W. and B. Subramanyam. 2010. Immature insects: ecological roles of mobility. Am. Entomol. 56: 230–241.

Hakim, R. S. 1976. Structural changes occurring during transformation of the labial gland cells to their adult form, in *Manduca sexta*. J. Morphol. 149: 547–565.

Hasenfuss, I., and N. P. Kristensen. 2003. Skeleton and muscles: immatures, pp. 133–164. *In* N. P. Kristensen (ed.), Lepidoptera: moths and butterflies 2. Handbuch der zoologie/Handbook of zoology IV/36. Walther de Gruyter, Berlin, Germany.

Heinrich, C. 1916. On the taxonomic value of some larval characters in the Lepidoptera. Proc. Entomol. Soc. Wash. 18: 154–164.

Helm, E. 1876. Über die Spinndrüsen der Lepidopteren. Wilhelm Engelmann, Leipzig, Germany. pp. 39.

Hinton, H. E. 1958. The phylogeny of the panorpoid orders. Annu. Rev. Entomol. 3: 181–206.

Huang, K., C. F. Li, J. Wu, J. H. Wei, Y. Zou, M. J. Han, and Z. Y. Zhou. 2016. Enhancer activity of Helitron in sericin-1 gene promoter from *Bombyx mori*. Insect Sci. 23: 396–405.

Inoue, S., K. Tanaka, F. Arisaka, S. Kimura, K. Ohtomo, and S. Mizuno. 2000. Silk fibroin of *Bombyx mori* is secreted, assembling a high molecular mass elementary unit consisting of H-chain, L-chain, and P25, with a 6: 6: 1 molar ratio. J. Biol. Chem. 275: 40517–40528.

International Silkworm Genome Consortium. 2008. The genome of a lepidopteran model insect, the silkworm *Bombyx mori*. Insect. Biochem. Mol. Biol. 38: 1036–1045.

Kanost, M. R., E. L. Arrese, X. Cao, Y.-R. Chen, S. Chellapilla, M. R. Goldsmith, E. Grosse-Wilde, D. G. Heckel, N. Herndon, H. Jiang, et al. 2016. Multifaceted biological insights from a draft genome sequence of the tobacco hornworm moth, *Manduca sexta*. Insect. Biochem. Mol. Biol. 76: 118–147.

Kent, K. S., J. G. Hildebrand, and T. N. Wiesel. 1987. Cephalic sensory pathways in the central nervous system of larval *Manduca sexta* (Lepidoptera: Sphingidae). Philos. Trans. R. Soc. Lond. B. Biol. Sci. 315: 1–36.

Koenig, C., A. Bretschneider, D. G. Heckel, E. Grosse-Wilde, B. S. Hansson, and H. Vogel. 2015. The plastic response of *Manduca sexta* to host and non-host plants. Insect. Biochem. Mol. Biol. 63: 72–85.

Kristensen, N. P. 1999. Lepidoptera: moths and butterflies 1. Handbuch der zoologie IV, vol. 35. Walther de Gruyter, Berlin, Germany. pp. 491.

Leslie, R. A., and H. A. Robertson. 1973. The structure of the salivary gland of the moth (*Manduca sexta*). Zeitschrift für Zellforschung und Mikroskopische Anatomie. 146: 553–564.

MacKay, M. R. 1964. The relationship of form and function of minute characters of lepidopterous larvae, and its importance in life-history studies. The Canadian Entomologist. 96: 991–1004.

Madden, T. 2002. The BLAST sequence analysis tool. *In* J. McEntyre and J. Ostell (eds.), The NCBI handbook [Internet]. National Center for Biotechnology Information (US), Bethesda, MD. Chapter 16. http://www.ncbi.nlm.nih.gov/books/NBK21097/

Ou, J., H. M. Deng, S. C. Zheng, L. H. Huang, Q. L. Feng, and L. Liu. 2014. Transcriptomic analysis of developmental features of *Bombyx mori* wing disc during metamorphosis. BMC Genomics 15: 820.

Paudel, S., I. Mikó, A. Deans, E. Rajotte, and G. Felton. 2018. Lyonet's gland of the tomato fruitworm, *Helicoverpa zea* (Lepidoptera: Noctuidae). PeerJ Preprints 6: e26455v1.

Perović, D. J., M. L. Johnson, B. Scholz, and M. P. Zalucki. 2008. The mortality of *Helicoverpa armigera* (Hübner) (Lepidoptera: Noctuidae) neonate larvae in relation to drop-off and soil surface temperature: the dangers of bungy jumping. Aust. J. Entomol. 47: 289–296.

Peterson, A. 1912. Anatomy of the tomato-worm larva, *Protoparce carolina*. Ann. Entomol. Soc. Am. 5: 246–269.

Rebers, J. E., and L. M. Riddiford. 1988. Structure and expression of a *Manduca sexta* larval cuticle gene homologous to *Drosophila* cuticle genes. J. Mol. Biol. 203: 411–423.

Reinecke, J. P., J. S. Buckner, and S. R. Grugel. 1980. Life cycle of laboratory-reared tobacco hornworms, *Manduca sexta*, a study of development and behavior, using time-lapse cinematography. BioI. Bull. 158: 129–140.

Ripley, L. B. 1924. The external morphology and postembryology of noctuid larvae. Ill. Biol. Monogr. 8: 1–102.

Rivera-Vega, L. J., D. A. Galbraith, C. M. Grozinger, and G. W. Felton. 2017a. Host plant driven transcriptome plasticity in the salivary glands of the cabbage looper (*Trichoplusia ni*). PLoS One 12: e0182636.

Rivera-Vega, L. J., F. E. Acevedo, and G. W. Felton. 2017b. Genomics of Lepidoptera saliva reveals function in herbivory. Curr. Opin. Insect Sci. 19: 61–69.

Rountree, D. B., and W. E. Bollenbacher. 1986. The release of the prothoracicotropic hormone in the tobacco hornworm, *Manduca sexta*, is controlled intrinsically by juvenile hormone. J. Exp. Biol. 120: 41–58.

Schindelin, J., I. Arganda-Carreras, E. Frise, V. Kaynig, M. Longair, T. Pietzsch, S. Preibisch, C. Rueden, S. Saalfeld, B. Schmid, et al. 2012. Fiji: an open-source platform for biological-image analysis. Nat. Methods 9: 676–682.

Sorensen, G. S., B. W. Cribb, D. Merritt, M-L. Johnson, and M. P. Zalucki. 2006. Structure and ultrastructure of the silk glands and spinneret of

Helicoverpa armigera (Hübner) (Lepidoptera: Noctuidae). Arthropod. Struct. Dev. 35: 3–13.

Tanaka, K., and S. Mizuno. 2001. Homologues of fibroin L-chain and P25 of *Bombyx mori* are present in *Dendrolimus spectabilis* and *Papilio xuthus* but not detectable in *Antheraea yamamai*. Insect. Biochem. Mol. Biol. 31: 665–677.

Tolbert, L. P., S. G. Matsumoto, and J. G. Hildebrand. 1983. Development of synapses in the antennal lobes of the moth *Manduca sexta* during metamorphosis. J. Neurosci. 3: 1158–1175.

Torres-Vila, L. M., J. Stockel, R. Roehrich, and M. C. Rodríguez-Molina. 1997. The relation between dispersal and survival of *Lobesia botrana* larvae and their density in vine inflorescences. Entomol. Exp. Appl. 84: 109–114.

Vegliante, F., and I. Hasenfuss. 2012. Morphology and diversity of exocrine glands in lepidopteran larvae. Annu. Rev. Entomol. 57: 187–204.

Wang, X., Y. Li, L. Peng, H. Chen, Q. Xia, and P. Zhao. 2016. Comparative transcriptome analysis of *Bombyx mori* spinnerets and Filippi's glands suggests their role in silk fiber formation. Insect. Biochem. Mol. Biol. 68: 89–99.

Wang, X., Y. Li, Q. Liu, X. Tan, X. Xie, Q. Xia, and P. Zhao. 2019. GC/MS-based metabolomics analysis reveals active fatty acids biosynthesis in the Filippi's gland of the silkworm, *Bombyx mori*, during silk spinning. Insect. Biochem. Mol. Biol. 105: 1–9.

Yamaguchi, K., Y. Kikuchi, T. Takagi, A. Kikuchi, F. Oyama, K. Shimura, and S. Mizuno. 1989. Primary structure of the silk fibroin light chain determined by cDNA sequencing and peptide analysis. J. Mol. Biol. 210: 127–139.

Yonemura, N., and F. Sehnal. 2006. The design of silk fiber composition in moths has been conserved for more than 150 million years. J. Mol. Evol. 63: 42–53.

Yonemura, N., F. Sehnal, K. Mita, and T. Tamura. 2006. Protein composition of silk filaments spun under water by caddisfly larvae. Biomacromolecules 7: 3370–3378.

Yonemura, N., K. Mita, T. Tamura, and F. Sehnal. 2009. Conservation of silk genes in Trichoptera and Lepidoptera. J. Mol. Evol. 68: 641–653.

Zhou, C., X. Zha, P. Shi, P. Wei, H. Wang, R. Zheng, and Q. Xia. 2016. Multiprotein bridging factor 2 regulates the expression of the fibroin heavy chain gene by interacting with Bmdimmed in the silkworm *Bombyx mori*. Insect. Mol. Biol. 25: 509–518.

Žurovec, M., and F. Sehnal. 2002. Unique molecular architecture of silk fibroin in the waxmoth, *Galleria mellonella*. J. Biol. Chem. 277: 22639–22647.

Žurovec, M., M. Vašková, D. Kodrík, F. Sehnal, and A. K. Kumaran. 1995. Light-chain fibroin of *Galleria mellonella* L. Mol. Gen. Genet. 247: 1–6.